JACS
JOURNAL OF THE AMERICAN CHEMICAL SOCIETY
Article
pubs.acs.org/JACS

# Negative Ion Photoelectron Spectroscopy Confirms the Prediction that 1,2,4,5-Tetraoxatetramethylenebenzene Has a Singlet Ground State

David A. Hrovat,[†] Gao-Lei Hou,[‡] Xue-Bin Wang,*[,‡] and Weston Thatcher Borden*[,†]

[†]Department of Chemistry and the Center for Advanced Scientific Computing and Modeling, University of North Texas, 1155 Union Circle, #305070, Denton, Texas 76203-5017, United States

[‡]Physical Sciences Division, Pacific Northwest National Laboratory, P.O. Box 999, MS K8-88, Richland, Washington 99352, United States

Supporting Information

**ABSTRACT:** The negative ion photoelectron (NIPE) spectrum of 1,2,4,5-tetraoxatetramethylenebenzene radical anion (**TOTMB**$^{\bullet-}$) shows that, like the hydrocarbon, 1,2,4,5-tetramethylenebenzene (**TMB**), the **TOTMB** diradical has a singlet ground state and thus violates Hund's rule. The NIPE spectrum of **TOTMB**$^{\bullet-}$ gives a value of $-\Delta E_{ST}$ = 3.5 ± 0.2 kcal/mol for the energy difference between the singlet and triplet states of **TOTMB** and a value of *EA* = 4.025 ± 0.010 eV for the electron affinity of **TOTMB**. (10/10)CASPT2 calculations are successful in predicting the singlet−triplet energy difference in **TOTMB** almost exactly, giving a computed value of $-\Delta E_{ST}$ = 3.6 kcal/mol. The same type of calculations predict $-\Delta E_{ST}$ = 6.1−6.3 kcal/mol in **TMB**. Thus, the calculated effect of the substitution of the four oxygens in **TOTMB** for the four methylene groups in **TMB** is very unusual, since the singlet state is selectively destabilized relative to the triplet state. The reason why **TMB** → **TOTMB** is predicted to result in a decrease in the size of $-\Delta E_{ST}$ is discussed.

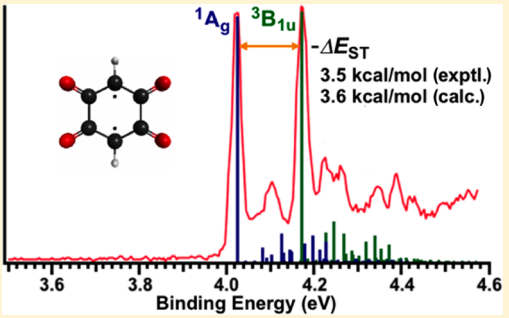


## INTRODUCTION

Negative ion photoelectron spectroscopy (NIPES)[1] has shown that the substitution of the oxygen atom in oxyallyl (**OXA**) for one methylene group in trimethylenemethane (**TMM**) has a huge effect on the relative energies of the lowest singlet and triplet states.[2] NIPES experiments by Lineberger and co-workers found that the triplet ground state of **TMM** is lower in energy than the lowest accessible singlet state by $\Delta E_{ST}$ = 16.2 kcal/mol.[3] In contrast, NIPES revealed that **OXA** has a singlet ground state, with the triplet higher in energy by $\Delta E_{ST}$ = −1.3 kcal/mol.[2] Thus, replacement of one $CH_2$ group in **TMM** by the oxygen in **OXA** selectively stabilizes the singlet, relative to the triplet, by 17.5 kcal/mol.

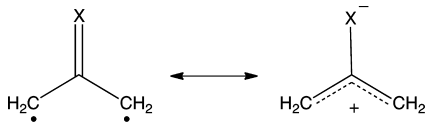


**TMM**, X = $CH_2$
**OXA**, X = O

A change in $\Delta E_{ST}$ of about this size between **TMM** and **OXA** had been predicted many years previously.[4] The predicted change in $\Delta E_{ST}$ was attributed to two factors. First, the greater strength of C═O, relative to C═C $\pi$ bonds, makes the resonance structure on the left dominant in both the singlet and triplet states of **OXA**. Second, the greater electronegativity of O, relative to $CH_2$, selectively stabilizes one of the two nonbonding MOs of **OXA**, which are degenerate in energy in **TMM**. The higher occupancy of the lower energy MO in singlet **OXA** than in triplet **OXA** makes the zwitterionic resonance structure on the right more important in the singlet than in the triplet state.[5]

In contrast to the case in **OXA**, NIPES has found that the effect on $\Delta E_{ST}$ of the substitution of oxygen atoms for both $CH_2$ groups in *meta*-benzoquinodimethane (**MBQDM**) is surprisingly small.[7] Lineberger and co-workers measured $\Delta E_{ST}$ = 9.6 kcal/mol in **MBQDM**,[8] which is reduced by only 0.6 kcal/mol, to $\Delta E_{ST}$ = 9.0 kcal/mol, in *meta*-benzoquinone (**MBQ**).[7,9] The reason why the change in $\Delta E_{ST}$ is so small is that, as had been predicted two decades earlier,[10] the lowest singlet state changes from $^1A_1$ in **MBQDM** (where preserving the aromaticity of the benzene ring is the dominant effect) to $^1B_2$ in **MBQ** (where the greater strength of the C═O $\pi$ bonds is the dominant effect). The relative energies of the $^1A_1$ and $^1B_2$ states change by 19.5 kcal/mol on going from **MBQDM** to **MBQ**, but the energy difference between the lower of these two states and the triplet decreases by only 0.6 kcal/mol.[7]

**Received:** April 28, 2015
**Published:** July 14, 2015





DOI: 10.1021/jacs.5b04416
J. Am. Chem. Soc. 2015, 137, 9094−9099

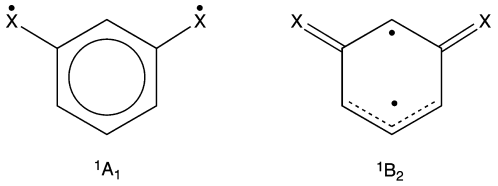


**MBQDM**, X = $CH_2$
**MBQ**, X = O

In this paper we report the use of NIPES to measure the value of $\Delta E_{ST}$ in the 1,2,4,5-tetraoxo derivative of 1,2,4,5-tetramethylenebenzene (**TMB**). Like **TMM** and **MBQDM**, **TMB** (more correctly named 2,3,5,6-tetramethylenecyclohexane-1,4-diyl) is a non-Kekulé hydrocarbon diradical.[11] The nonbonding (NB)MOs of **TMB** can be chosen to be the NBMOs of two pentadienyl radicals, so that, unlike the case in **TMM** or in **MBQDM**, the NBMOs have no atoms in common.[12] Since the NBMOs of **TMB** can be chosen to be disjoint, to a first approximation, the lowest singlet and triplet states of **TMB** would be expected to have the same energies.[13]

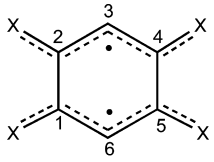


**TMB**, X = $CH_2$
**TOTMB**, X = O

However, 1,4-bonding interactions between the large positive spin densities at C3−C6 and at the four methylene groups and 1,2-bonding interactions between the smaller negative spin densities at C1−C2 and C4−C5 were predicted to make the singlet the ground state of **TMB**.[12] Initial experiments by the group of the late Professor Wolfgang Roth appeared to show that this prediction was incorrect and that the triplet is the ground state of **TMB**.[14] Nevertheless, subsequent experiments by Berson and co-workers revealed that **TMB** does, in fact, have a singlet ground state.[15,16] Thus, **TMB** represents a rare example of a diradical that, by having a singlet ground state, violates Hund's rule.[17]

Although it is now known that **TMB** does, in fact, have a singlet ground state,[15,16] the value of $\Delta E_{ST}$ in **TMB** has not been measured. In this paper we report the measurement of $\Delta E_{ST}$ in a heteroatom derivative, 1,2,4,5-tetraoxa (**TO**)**TMB**, by NIPES. The NIPE spectrum of **TOTMB**$^{\bullet-}$ shows that, like **TMB**, **TOTMB** has a singlet ground state and thus violates Hund's rule.[17]

We also report the results of electronic structure calculations that reproduce the NIPES value of $\Delta E_{ST}$ in **TOTMB** with almost perfect accuracy. We have carried out exactly the same type of calculations on **TMB**; so we argue that the value of $\Delta E_{ST}$ in **TMB** thus obtained is also likely to be very accurate. Interestingly, the calculations on **TMB** and **TOTMB** predict that, in stark contrast to the case in **TMM** → **OXA**,[2] substitution of the four methylene groups in **TMB** by the four oxygens in **TOTMB** actually destabilizes the singlet state, relative to the triplet. This computational finding is discussed and rationalized.

## METHODOLOGY, RESULTS, AND DISCUSSION

**Generation and NIPE Spectroscopy of TOTMB$^{\bullet-}$.** We were able to obtain NIPE spectra of the radical anion of **TOTMB** (**TOTMB**$^{\bullet-}$) by taking advantage of the acidifying effect of the four oxygens in 2,5-dihydroxy-1,4-benzoquinone (**DHBQ**). Formation of the dianion (**DHBQ**$^{2-}$) in solution, followed by transfer of the dianion into the gas phase by electrospray, led to spontaneous loss of an electron and formation of **TOTMB**$^{\bullet-}$ (Scheme 1).

**Scheme 1**

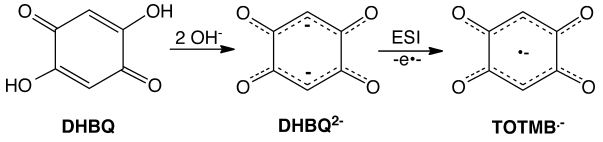


The NIPE spectra of **TOTMB**$^{\bullet-}$ were obtained with a low-temperature, magnetic-bottle NIPE spectrometer, coupled to an electrospray ion source (ESI) and a cryogenic ion trap.[18] The **TOTMB** radical anions were generated by electrospraying into the gas phase a 0.1 mM solution of **DHBQ**, dissolved in water/acetonitrile, to which a dilute aqueous solution of NaOH was added dropwise, in order to optimize the **TOTMB**$^{\bullet-}$ intensity.

The **TOTMB** radical anions formed were directed by quadrupole ion guides into a cryogenic ion trap. The cooling of the radical anions to 20 K eliminated the possibility of appearance of extra spectral peaks in the NIPE spectrum, due to hot bands. The cooled radical anions were transferred into a time-of-flight mass spectrometer.

**DHBQ**$^{2-}$ dianions were not observed in the mass spectrometer, because they are electronically unstable species in the gas-phase, with negative electron binding energies. The unbound electron spontaneously autodetaches in the gas phase, leading to formation of the singly charged, **TOTMB**$^{\bullet-}$, radical monoanions.

In addition to **TOTMB**$^{\bullet-}$, singly deprotonated **DHBQ** anions were concurrently generated, and they have $m/z$ = 139, which is only 1 amu larger than that of **TOTMB**$^{\bullet-}$. Therefore, the **TOTMB** radical anions were carefully mass selected, before being intersected by a Nd:YAG laser (266 nm; 4.661 eV) or a ArF laser (193 nm; 6.424 eV) in the photodetachment zone of the magnetic-bottle, photoelectron analyzer. Photoelectrons were collected at nearly 100% efficiency.

The best instrumental resolution was 20 meV full width at half-maximum (fwhm) for electrons with 1 eV of kinetic energy, as demonstrated, after maximum ion deceleration, by the NIPE spectrum of $I^-$. However, due to the modest mass intensity of **TOTMB**$^{\bullet-}$, the NIPE spectra of **TOTMB**$^{\bullet-}$ were obtained with less optimal resolutions of 30 meV for 1 eV kinetic energy electrons.

Figure 1 shows the 20 K NIPE spectrum of **TOTMB**$^{\bullet-}$ at 266 nm. The NIPE spectrum at 193 nm, which is provided in Figure S1 of the Supporting Information (SI), shows the same set of peaks with electron binding energies (EBEs) of 4.0−4.6 eV as in the 266 nm spectrum. However, additional peaks are seen at EBE = 4.63 and 5.06 eV in the 193 nm NIPE spectrum.

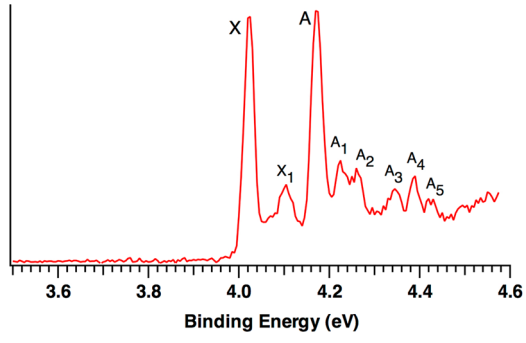


**Figure 1.** The 20 K NIPE spectrum of **TOTMB**$^{\bullet-}$ at 266 nm (4.661 eV). The origins of the bands for what appear to be the first two electronic states of **TOTMB** are marked X and A.



DOI: 10.1021/jacs.5b04416
J. Am. Chem. Soc. 2015, 137, 9094−9099

Table 1. Calculated and Experimental Values of the EA and the Singlet−Triplet Energy Difference ($\Delta E_{ST}$) in TOTMB

| method | EA (eV)[a] | $-\Delta E_{ST}$ (kcal/mol)[b] |
|---|---|---|
| UB3LYP/aug-cc-pVTZ//UB3LYP/aug-cc-pVTZ[c] | 4.12[d] | 5.2[e] |
| CASPT2/aug-cc-pVDZ//CASSCF/aug-cc-pVDZ | 4.12 | 3.6 |
| CASPT2/aug-cc-pVDZ//CASPT2/aug-cc-pVDZ | 4.16 | 3.4 |
| CASPT2/aug-cc-pVTZ//CASPT2/aug-cc-pVDZ | 4.28 | 3.6 |
| CASPT2/aug-cc-pVQZ//CASPT2/aug-cc-pVDZ | 4.34 | 3.6 |
| NIPES | 4.025 ± 0.010 | 3.5 ± 0.2 |

[a]Adiabatic EA. [b]Negative sign for $\Delta E_{ST}$ indicates that the singlet is lower in energy than the triplet. [c]Using a broken symmetry wave function with $S^2$ = 0.98 for the lowest singlet state. [d]Before correction for spin contamination of the singlet wave function by the triplet,[27] EA = 4.23 eV. [e]Before correction for spin contamination of the singlet wave function by the triplet,[27] $-\Delta E_{ST}$ = 2.7 kcal/mol.

The well-resolved spectral peaks in Figure 1 correspond to transitions from the ground state of **TOTMB**$^{\bullet-}$ to the ground and excited states of **TOTMB**, along with the vibrational excitations that are associated with formation of each electronic state of **TOTMB**. The two sharp, strong peaks, X and A, at EBE = 4.025 and 4.175 eV, respectively, are assigned as the origins of the first two electronic states of **TOTMB**. The EBEs of all of the peaks in Figure 1 are 4.025 (X), 4.105 ($X_1$), 4.175 (A), 4.225 ($A_1$), 4.260 ($A_2$), 4.345 ($A_3$), 4.390 ($A_4$), and 4.430 eV ($A_5$).

As shown in Figure 1, the intensity of peak X is marginally smaller than that of peak A in the 266 nm NIPE spectrum, and the intensity of X is ca. 30% smaller than that of A in the 193 nm spectrum (Figure S1 of the SI). Unless the geometry of the triplet state differs much more than that of the lowest singlet state from the geometry of the radical anion, spin statistics make the peak for formation of the triplet the more intense peak in NIPE spectra.[1] Therefore, since the geometries of the lowest singlet and triplet states of **TOTMB** are predicted to be nearly the same (vide infra), the NIPE spectra of **TOTMB**$^{\bullet-}$ indicate that peak A is for formation of the triplet state of **TOTMB** and peak X is for formation of the lowest singlet state. Thus, the NIPE spectra of **TOTMB**$^{\bullet-}$ indicate that, as is the case in **TMB**,[15,16] a singlet is the ground state of **TOTMB**.

The adiabatic detachment energy (ADE) of **TOTMB**$^{\bullet-}$ [i.e., the electron affinity (EA) of **TOTMB**] is determined from the position of peak X to be 4.025 ± 0.010 eV. The EBE difference between peaks X and A in Figure 1 corresponds to the energy difference between the lowest singlet and triplet electronic states of **TOTMB**. $\Delta E_{ST}$ = −0.15 ± 0.01 eV = −3.5 ± 0.2 kcal/mol is obtained from the NIPE spectrum in Figure 1.

**Electronic Structure Calculations.** The assignment of peaks X and A in Figure 1 as belonging to, respectively, the lowest singlet and triplet states of **TOTMB** is strongly supported by the results of electronic structure calculations. DFT calculations were performed with the B3LYP hybrid functional,[19−21] using the augmented cc-pVTZ basis set.[22] Geometries were optimized and vibrational frequencies were computed at this level of theory using the Gaussian09 suite of programs.[23]

Wave function-based calculations were also performed. They consisted of CASSCF calculations, for which configurations were generated by distributing all 10 $\pi$ electrons among the 10 lowest-energy $\pi$ MOs. The orbitals from the (10/10)CASSCF calculations served as the input for (10/10)CASPT2 calculations.[24] The CASPT2 calculations include the effects of dynamic electron correlation[25] that are missing from the CASSCF calculations.

The (10/10)CASPT2 calculations were performed with augmented, correlation-consistent basis sets, ranging from aug-cc-pVDZ to aug-cc-pVQZ.[22] Geometries were optimized and vibrational frequencies were computed at both the (10/10)CASSCF and (10/10)CASPT2 levels of theory using the aug-cc-pVDZ basis set. The CASSCF and CASPT2 calculations were performed using MOLCAS Version 8.0.[26]

Table 1 summarizes our calculated values of EA and $\Delta E_{ST}$ for **TOTMB** and compares them to the experimental values, obtained from the NIPE spectrum of **TOTMB**$^{\bullet-}$. As shown in Table 1, all of the computed EA values are too high by 0.1−0.3 eV, but CASPT2 gives values of $\Delta E_{ST}$ that are in almost perfect agreement with the experimental value.

Further evidence of the congruence between the computed and observed NIPE spectrum of **TOTMB**$^{\bullet-}$ comes from the comparisons in Figure 2 of the vibrational bands in the simulated NIPE spectrum

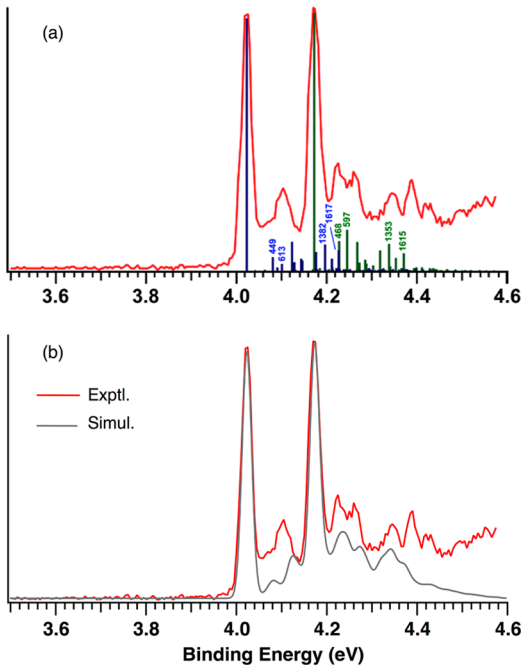


Figure 2. (a) CASPT2/aug-cc-pVDZ calculated vibrational structure in the NIPE spectrum of **TOTMB**$^{\bullet-}$, superimposed on the experimental NIPE spectrum (red). Frequencies ($cm^{-1}$) for symmetrical vibrational modes are shown for each state. (See Figure S2 of the SI for mode assignments). The positions of the bands in the calculated spectrum have been adjusted by −0.09 eV for both the singlet (blue) and triplet (green), in order to align the 0,0 bands in the calculated spectrum with the 0,0 bands in the observed spectrum. (b) Convoluted spectrum (gray), using Gaussian line shapes with 25 meV fwhm for each stick in (a), superimposed on the experimental 266 spectrum (red). The convoluted spectrum was obtained by multiplying the Gaussians by the FCFs for the singlet and 1.15 times the FCFs for the triplet and summing.

with those in the actual 266 nm spectrum. The simulated spectrum was generated by using the results of the CASPT2/aug-cc-pVDZ vibrational analyses to compute the Franck−Condon factors[28] for the vibrational bands in the peaks for formation of the $^1A_g$ and $^3B_{1u}$ states of **TOTMB** from the $^2B_{2g}$ state of **TOTMB**$^{\bullet-}$.[29] The ezSpectrum program[30] was used to calculate the intensity of each of the vibrational bands in the NIPE spectrum. The optimized geometries, unscaled harmonic vibrational frequencies, and normal mode vectors from the CASPT2/aug-cc-pVDZ calculations were used as the input to ezSpectrum, and Duschinsky rotations[31] were included in the calculated intensities.



DOI: 10.1021/jacs.5b04416
J. Am. Chem. Soc. 2015, 137, 9094−9099

In superimposing the positions and intensities of the vibrational bands in the calculated CASPT2/aug-cc-pVDZ NIPE spectrum of **TOTMB**$^{\bullet-}$ onto the 266 nm NIPE spectrum, the positions of the computed 0,0 bands were adjusted. Table 1 shows that the calculated value of EA at this level of theory is 0.09 eV higher than the experimental value. Therefore, the positions of all of the calculated vibrational bands in the singlet and triplet state of **TOTMB** were decreased by this amount of energy. The resulting stick spectrum is shown in Figure 2a.

The calculated NIPE spectra, convoluted with a Gaussian line shape for each stick in Figure 2a, were generated and superimposed on the experimental 266 nm spectrum. A series of different Gaussians (fwhm = 25, 20, and 30 meV) was used. The resulting spectra are shown in Figures S3−S5. These three simulated spectra are similar to each other, but the one with a simulated resolution of fwhm = 25 meV in Figure S3 best fits the experimental spectrum in terms of reproducing the main spectral peak widths. This simulated NIPE spectrum is shown in Figure 2b.

The simulations provide a good fit for almost all of the observed vibrational fine structure. However, starting with EBE > 4.3 eV, the peaks in the experimental NIPE spectrum seem to sit on top of a background, which makes these peaks appear more intense than they would be if only direct detachment processes were involved. Resonant photodetachment[32] may give rise to an underlying band in this region of the NIPE spectrum, which could account for the differences in Figure 2 between the calculated and observed intensities of the bands in this region of the spectrum (e.g., in the band with EBE = 4.39 eV).

Comparisons of the calculated frequencies of the vibrational bands that are active in the NIPE spectrum of **TOTMB**$^{\bullet-}$ in Figure 2a show that the frequencies of these bands are very similar in the singlet and triplet regions of the spectrum. The calculated bond lengths in these two states are also very similar. The bond lengths, optimized at three different levels of theory, are given in Figure 3.

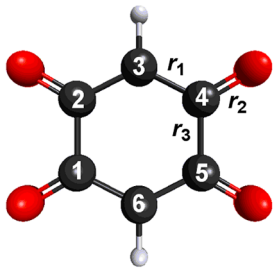


| | CASPT2 | | | CASSCF | | | UB3LYP | | |
|---|---|---|---|---|---|---|---|---|---|
| | $^2B_{2g}$ | $^1A_g$ | $^3B_{1u}$ | $^2B_{2g}$ | $^1A_g$ | $^3B_{1u}$ | $^2B_{2g}$ | $^1A_g$ | $^3B_{1u}$ |
| $r_1$ | 1.446 | 1.457 | 1.458 | 1.438 | 1.452 | 1.454 | 1.431 | 1.445 | 1.446 |
| $r_2$ | 1.249 | 1.236 | 1.236 | 1.225 | 1.218 | 1.216 | 1.232 | 1.221 | 1.220 |
| $r_3$ | 1.530 | 1.533 | 1.543 | 1.510 | 1.517 | 1.524 | 1.535 | 1.538 | 1.549 |

**Figure 3.** Calculated bond lengths (Å) in the $^2B_{2g}$ state of **TOTMB**$^{\bullet-}$ and in the $^1A_g$ and $^3B_{1u}$ states of **TOTMB**, optimized at three different levels of theory using the aug-cc-pVDZ (CASSCF and CASPT2) and aug-cc-pVTZ (B3LYP) basis sets.

The fact that the vibrational frequencies and C−C bond lengths in the singlet and triplet states of **TOTMB** are very similar is not surprising, because both states can be described as consisting of two 1,5-dioxapentadienyl radicals, which interact only weakly. However, the 0.007−0.011 Å shorter C1−C2 and C4−C5 bond lengths ($r_3$) in the singlet than in the triplet indicate that the weak interactions between the 1,5-dioxapentadienyl radicals in **TOTMB** provide more bonding in the singlet than in the triplet. This is, presumably, the reason why the singlet is the ground state of **TOTMB**.

There are two types of weak interactions between the dioxapentadienyl radicals in **TOTMB**. The first type consists of the 1,4-interactions between the pairs of atoms where unpaired spin appears (i.e., the central carbons and the oxygen atoms of the two 1,5-dioxapentadienyl radicals). These 1,4-interactions, which occur between electrons of opposite spin in the singlet state, are bonding in this state, but not in the triplet state, where the interactions involve electrons of the same spin.

In MO theory these 1,4-interactions make the in-phase ($b_{3u}$) combination of the two dioxapentadienyl nonbonding orbitals slightly lower in energy than the out-of-phase ($b_{2g}$) combination. Consequently, the in-phase combination has a slightly higher occupation number than the out-of-phase combination in the lowest singlet state; whereas, in the triplet state one electron occupies each of these MOs. Consequently, these 1,4-interactions stabilize the singlet but not the triplet state.

The size of this selective stabilization of the singlet state can be estimated by comparing the energy of a two-configuration (TC)SCF wave function for the singlet with an ROHF wave function for the triplet. The unequal occupation numbers of 1.29 electrons in the $b_{3u}$ MO and 0.71 electrons in the $b_{2g}$ MO are calculated to make the TCSCF singlet lower in energy than the ROHF triplet by 2.0 kcal/mol and to make the $r_3$ bond length 0.007 Å shorter in the singlet than in the triplet.

The remaining 1.6 kcal/mol of the calculated value of $-\Delta E_{ST}$ = 3.6 kcal/mol in **TOTMB** is attributable to the second type of weak interaction between the two dioxapentadienyl radicals in **TOTMB**. These interactions involve the negative spin densities at the nodal carbons (C1−C2 and C4−C5) of the two dioxapentadienyl radicals in **TOTMB**. Negative spin densities do not appear in the ROHF wave function for a monoradical or in the ROHF or TCSCF wave functions for a diradical. However, negative spin densities do appear in CASSCF and CASPT2 wave functions, where correlation between unpaired electrons in nonbonding MOs and electrons in bonding MOs is included.[33]

The electron spins in the 2p-$\pi$ AOs at these pairs of nodal carbons are parallel in the triplet but antiparallel in the singlet. Consequently, there should be more $\pi$ bonding between C1 and C2 and between C4 and C5 in singlet **TOTMB** than in the triplet, thus contributing to the shorter $r_3$ bond distances in the singlet than in the triplet. The greater $\pi$ bonding between these pairs of carbons in the singlet than in the triplet also contributes to the fact that, in violation of Hund's rule, the singlet is both calculated and found to be the ground state of **TOTMB**.

**Comparison with TMB.** If the $\pi$ systems of **TMB** and **TOTMB** can be described, respectively, as those of two weakly interacting pentadienyl radicals and two weakly interacting 1,5-dioxapentadienyl radicals, it follows that substitution of the four oxygens in **TOTMB** for the four methylene groups in **TMB** should have only a minor effect on $\Delta E_{ST}$. In fact, previous (10/10)CASPT2/6-31G*//(10/10)CASSCF/6-31G* calculations on **TMB** gave $-\Delta E_{ST}$ = 5.2 kcal/mol,[16] which is close to but slightly greater than the CASPT2 values of $-\Delta E_{ST}$ = 3.4−3.6 kcal/mol in Table 1 for **TOTMB**.

We decided to carry out calculations on **TMB** at exactly the same level of theory as the calculations in Table 1 on **TOTMB** for two reasons. The first is that the CASPT2 calculations in Table 1 provide computed values of $-\Delta E_{ST}$ in **TOTMB** that are in almost perfect agreement with the experimental values obtained by NIPES. Consequently, there is every reason to believe that the same type of calculations should provide an equally accurate predicted value of $-\Delta E_{ST}$ in **TMB**, a value that has not yet been measured.

Second, we wanted to know whether identical types of calculations would find that $-\Delta E_{ST}$ really is slightly larger in **TMB** than in **TOTMB**. This question is of interest because it would mean that, in stark contrast to the case in **TMM** → **OXA**,[2] the substitution of the four oxygens in **TOTMB** for the four terminal $CH_2$ groups in **TMB** actually destabilizes the singlet state, relative to the triplet state.

The results of our calculations of $-\Delta E_{ST}$ in **TMB** are given in Table 2. Comparison of the results in Table 2 with the results in Table 1 shows that the computed values of $-\Delta E_{ST}$ are about 70−80% higher in **TMB** than in **TOTMB**. Therefore, in **TMB** → **TOTMB** the substitution of oxygen for $CH_2$ really is predicted to destabilize the singlet state, relative to the lowest triplet state.

Also shown in Table 2 are calculated values of the EA in **TMB**. The fact that EA is computed to be positive means that **TMB**$^{\bullet-}$ should be


DOI: 10.1021/jacs.5b04416
J. Am. Chem. Soc. 2015, 137, 9094−9099

**Table 2. Calculated Values of the EA and the Singlet−Triplet Energy Difference ($\Delta E_{ST}$) in TMB**

| method | EA (eV)[a] | $-\Delta E_{ST}$ (kcal/mol)[b] |
|---|---|---|
| UB3LYP/aug-cc-pVTZ//UB3LYP/aug-cc-pVTZ[c] | 1.05[d] | 9.2[e] |
| CASPT2/aug-cc-pVDZ//CASSCF/aug-cc-pVDZ | 1.17 | 6.1 |
| CASPT2/aug-cc-pVDZ//CASPT2/aug-cc-pVDZ | 1.18 | 6.1 |
| CASPT2/aug-cc-pVTZ//CASPT2/aug-cc-pVDZ | 1.28 | 6.2 |
| CASPT2/aug-cc-pVQZ//CASPT2/aug-cc-pVDZ | 1.32 | 6.3 |

[a]Adiabatic EA. [b]Negative sign for $\Delta E_{ST}$ indicates that the singlet is lower in energy than the triplet. [c]Using a broken symmetry wave function with $S^2 = 0.98$ for the lowest singlet state. [d]Before correction for spin contamination of the singlet wave function by the triplet,[27] EA = 1.26 eV. [e]Before correction for spin contamination of the singlet wave function by the triplet,[27] $-\Delta E_{ST}$ = 4.4 kcal/mol.

bound. Therefore, NIPES can, at least in principle, be used to measure the singlet−triplet energy difference in **TMB** and to confirm the prediction that in **TMB** → **TOTMB**, the substitution of oxygen for $CH_2$ lowers, rather than raises, the value of $-\Delta E_{ST}$.

Why is the substitution of the four oxygens in **TOTMB** for the four methylene groups in **TMB** predicted to lower, rather than raise, the value of $-\Delta E_{ST}$? The results of TCSCF and ROHF calculations on **TMB** show that at this level of theory, the singlet is calculated to be lower in energy than the triplet by 2.0 kcal/mol, which is the same as the energy difference between these two states in **TOTMB**.[34] Consequently, the 2.6 kcal/mol lower CASPT2 values of $-\Delta E_{ST}$ in Table 1 for **TOTMB** than in Table 2 for **TMB** must be due to less bonding between the negative spin densities at the nodal carbons in the two 1,5-dioxapentadienyl radicals in singlet **TOTMB** than between the negative spin densities at the nodal carbons in the two pentadienyl radicals in singlet **TMB**.

Replacement of the $\pi$ bonds to the two terminal methylene groups of pentadienyl radical by the stronger C=O $\pi$ bonds in 1,5-dioxapentadienyl radical would be expected to increase the localization of the unpaired electron at the central carbon. Since it is the correlation between the unpaired electron and the electrons in the $\pi$ bonding MOs that gives rise to the negative spin densities in pentadienyl radical,[33] increasing the localization of the unpaired electron at the central carbon should decrease the amount of negative spin density at the two nodal carbons in 1,5-dioxapentadienyl radical, relative to that in pentadienyl radical. In fact, the results of the UB3LYP/aug-cc-pVTZ calculations, summarized in Figure 4, do show this to be the case.[35]

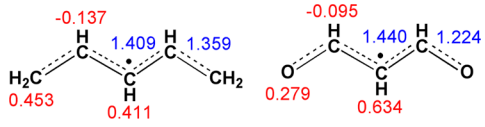


**Figure 4.** UB3LYP/aug-cc-pVTZ spin densities (red) and bond lengths (Å, blue) in pentadienyl (left) and 1,5-dioxapentadienyl (right) radicals. The greater localization of the unpaired electron in the latter radical is shown not only by the higher spin density at the central carbon but also by the longer C−C bonds to it. The greater localization of the unpaired electron is calculated to result in about a 50% reduction in the amount of negative spin density at the two nodal carbons in 1,5-dioxapentadienyl radical, compared to pentadienyl radical.

The smaller amounts of negative spin densities at the nodal carbons of 1,5-dioxapentadienyl radical than of pentadienyl radical explain why there is less $\pi$ bonding between the nodal carbons of the two 1,5-dioxapentadienyl radicals in **TOTMB** than between these carbons of the two pentadienyl radicals in **TMB**. Thus, it is the reduction in negative spin density at the nodal carbons, caused by the substitution of the four oxygens in **TOTMB** for the four $CH_2$ groups in **TMB**, that results in this substitution of O for $CH_2$ actually making the value of $-\Delta E_{ST}$ smaller in **TOTMB** than in **TMB**.

## CONCLUSIONS

The NIPE spectrum of **TOTMB**$^{\bullet-}$ shows that, like **TMB**,[15,16] the **TOTMB** diradical has a singlet ground state and thus violates Hund's rule.[17] From the NIPE spectrum, $-\Delta E_{ST}$ = 3.5 ± 0.2 kcal/mol in **TOTMB** is obtained. (10/10)CASPT2 calculations are successful in predicting this value of $-\Delta E_{ST}$ almost exactly.

The value of $-\Delta E_{ST}$ in the **TMB** hydrocarbon diradical has not yet been measured, but (10/10)CASPT2 calculations predict a value of $-\Delta E_{ST}$ = 6.1−6.3 kcal/mol. Given the high accuracy with which (10/10)CASPT2 predicts the value of $-\Delta E_{ST}$ in **TOTMB**, there is every reason to expect the (10/10)CASPT2 value of $-\Delta E_{ST}$ = 6.1−6.3 kcal/mol in **TMB** to be very accurate.

Although, the substitution of oxygen for one methylene group in **TMM** selectively stabilizes the singlet state of **OXA** by 17.5 kcal/mol,[2] in contrast, our (10/10)CASPT2 calculations predict that the substitution in **TOTMB** of all four methylene groups in **TMB** by oxygens has the opposite effect. In **TMB** → **TOTMB**, the singlet state is calculated to be selectively destabilized by 2.5−2.7 kcal/mol.

Since the system of **TMB** can be described as two pentadienyl radicals connected at nodal carbons, to a first approximation the substitution of the four oxygen atoms in **TOTMB** for the four methylene groups in **TMB** should have no effect on $\Delta E_{ST}$. However, the four oxygens in **TOTMB** increase the localization of the unpaired electrons at the two central carbons (C3 and C6), which reduces the amount of negative spin density at C1, C2, C4, and C5. It is bonding between the negative spins at these carbons that helps to make the singlet the ground state of both **TMB** and **TOTMB**. The reduction of the negative spin density at these four carbons in **TMB** by the four oxygens in **TOTMB** is the reason why **TOTMB** actually has a smaller predicted value of $-\Delta E_{ST}$ than **TMB**.

NIPES seems the most promising way to test our prediction that **TOTMB** has a 2.6 kcal/mol smaller value of $-\Delta E_{ST}$ than **TMB**. We hope that our prediction will serve to stimulate the measurement of the NIPE spectrum of **TMB**$^{\bullet-}$.

## ASSOCIATED CONTENT

### Supporting Information

The 20 K NIPE spectra of **TOTMB**$^{\bullet-}$ at 266 and 193 nm (Figure S1); frequency assignments of symmetric vibrational modes for the $^1A_g$ and $^3B_{1u}$ states of **TOTMB** (Figure S2); stick spectrum in Figure 2, convoluted using Gaussian line shapes with fwhm of 25, 20, and 30 meV, superimposed on the experimental 266 nm spectrum (Figures S3−S5); spin densities and bond lengths in **TMB** and **TOTMB** (Figure S6); and optimized geometries, vibrational frequencies, and energies for the $^1A_g$ and $^3B_{1u}$ states of **TOTMB** and **TMB** and the $^2B_{2g}$ state of **TOTMB**$^{\bullet-}$ and **TMB**$^{\bullet-}$. The Supporting Information is available free of charge on the ACS Publications website at DOI: 10.1021/jacs.5b04416.

## AUTHOR INFORMATION

### Corresponding Authors

*borden@unt.edu
*xuebin.wang@pnnl.gov



DOI: 10.1021/jacs.5b04416
J. Am. Chem. Soc. 2015, 137, 9094−9099

## Notes

The authors declare no competing financial interest.

## ■ ACKNOWLEDGMENTS

The calculations at UNT were supported in part by Grant CHE-0910527 from the National Science Foundation and by Grant B0027 from the Robert A. Welch Foundation. The NIPES research at PNNL was supported by the U.S. Department of Energy (DOE), Office of Science, Office of Basic Energy Sciences, Division of Chemical Sciences, Geosciences and Biosciences, and was performed at the EMSL, a national scientific user facility sponsored by DOE's Office of Biological and Environmental Research and located at Pacific Northwest National Laboratory.

## ■ REFERENCES

(1) Reviews: (a) Lineberger, L. C.; Borden, W. T. *Phys. Chem. Chem. Phys.* **2011**, *13*, 11792. (b) Borden, W. T. In *Fifty Years of the James Flack Norris Award*; Strom, E. T., Mainz, V., Eds.; American Chemical Society: Washington, DC, in press.

(2) (a) Ichino, T.; Villano, S. M.; Gianola, A. J.; Goebbert, D. J.; Velarde, L.; Sanov, A.; Blanksby, S. J.; Zhou, X.; Hrovat, D. A.; Borden, W. T.; Lineberger, W. C. *Angew. Chem., Int. Ed.* **2009**, *48*, 8509. (b) Ichino, T.; Villano, S. M.; Gianola, A. J.; Goebbert, D. J.; Velarde, L.; Sanov, A.; Blanksby, S. J.; Zhou, X.; Hrovat, D. A.; Borden, W. T.; Lineberger, W. C. *J. Phys. Chem. A* **2011**, *115*, 1634.

(3) (a) Wenthold, P. G.; Hu, J.; Squires, R. R.; Lineberger, W. C. *J. Am. Chem. Soc.* **1996**, *118*, 475. (b) Wenthold, P. G.; Hu, J.; Squires, R. R.; Lineberger, W. C. *J. Am. Soc. Mass Spectrom.* **1999**, *10*, 800.

(4) Coolidge, M. B.; Borden, W. T. *J. Am. Chem. Soc.* **1990**, *112*, 1704.

(5) However, calculations found the carbonyl group of singlet **OXA** not to be significantly more polar than the carbonyl group of acetone.[6] Experimental evidence, confirming the presence of a strong C═O $\pi$ bond in singlet **OXA**, was provided by a progression of 1680 ± 50 $cm^{-1}$ in the NIPE spectrum of $\mathbf{OXA}^{\bullet-}$, which was attributed to C═O stretching in the singlet state of **OXA**.[2]

(6) Lim, D.; Hrovat, D. A.; Borden, W. T.; Jorgensen, W. L. *J. Am. Chem. Soc.* **1994**, *116*, 3494.

(7) Chen, B.; Hrovat, D. A.; Deng, S. H. M.; Zhang, J.; Wang, X.-B.; Borden, W. T. *J. Am. Chem. Soc.* **2014**, *136*, 3589.

(8) Wenthold, P. G.; Kim, J. B.; Lineberger, W. C. *J. Am. Chem. Soc.* **1997**, *119*, 1354.

(9) Fu, Q.; Yang, J.; Wang, X.-B. *J. Phys. Chem. A* **2011**, *115*, 3201.

(10) Fort, R. C., Jr.; Getty, S. J.; Hrovat, D. A.; Lahti, P. M.; Borden, W. T. *J. Am. Chem. Soc.* **1992**, *114*, 7549.

(11) Review: Berson, J. A. In *Reactive Intermediate Chemistry*; Moss, R. A., Platz, M. S., Jones, M., Jr., Eds.; Wiley Interscience: Hoboken, NJ, 2004; pp 165−203.

(12) Du, P.; Hrovat, D. A.; Borden, W. T.; Lahti, P. M.; Rossi, A. R.; Berson, J. A. *J. Am. Chem. Soc.* **1986**, *108*, 5072.

(13) (a) Borden, W. T.; Davidson, E. R. *J. Am. Chem. Soc.* **1977**, *99*, 4587. (b) Borden, W. T. In *Diradicals*; Borden, W. T., Ed.; Wiley-Interscience: New York, 1982; pp 1−72.

(14) (a) Roth, W. R.; Longer, R.; Bartmann, M.; Stevermann, B.; Maier, G.; Reisenauer, H. P.; Sustmann, R.; Müller, W. *Angew. Chem., Int. Ed. Engl.* **1987**, *26*, 256. (b) Roth, W. R.; Langer, R.; Ebbrecht, T.; Beitat, A.; Lennartz, H.-W. *Chem. Ber.* **1991**, *124*, 2751.

(15) (a) Reynolds, J. H.; Berson, J. A.; Kumashiro, K. K.; Duchamp, J. C.; Zilm, K. W.; Rubello, A.; Vogel, P. *J. Am. Chem. Soc.* **1992**, *114*, 763. (b) Reynolds, J. H.; Berson, J. A.; Scaiano, J. C.; Berinstain, A. B. *J. Am. Chem. Soc.* **1992**, *114*, 5866. (c) Reynolds, J. H.; Berson, J. A.; Kumashiro, K. K.; Duchamp, J. C.; Zilm, K. W.; Scaiano, J. C.; Berinstain, A. B.; Rubello, A.; Vogel, P. *J. Am. Chem. Soc.* **1993**, *115*, 8073.

(16) See also Hrovat, D. A.; Borden, W. T. *J. Am. Chem. Soc.* **1994**, *116*, 6327.

(17) Reviews: (a) Borden, W. T.; Iwamura, H.; Berson, J. A. *Acc. Chem. Res.* **1994**, *27*, 109. (b) Kutzelnigg, W. *Angew. Chem., Int. Ed. Engl.* **1996**, *35*, 572. (c) Hrovat, D. A.; Borden, W. T. In *Modern Electronic Structure Theory and Applications in Organic Chemistry*; Davidson, E. R., Ed.; World Scientific Publishing Company: Singapore, 1997; pp 171−195.

(18) Wang, X.-B.; Wang, L.-S. *Rev. Sci. Instrum.* **2008**, *79*, 073108.

(19) B3LYP is a combination of Becke's 3-parameter hybrid exchange functional (B3)[20] with the electron correlation functional of Lee, Yang, and Parr (LYP).[21]

(20) Becke, A. D. *J. Chem. Phys.* **1993**, *98*, 5648.

(21) Lee, C.; Yang, W.; Parr, R. G. *Phys. Rev. B: Condens. Matter Mater. Phys.* **1988**, *37*, 785.

(22) (a) Dunning, T. H. *J. Chem. Phys.* **1989**, *90*, 1007. (b) Kendall, R. A.; Dunning, T. H.; Harrison, R. J. *J. Chem. Phys.* **1992**, *96*, 6796.

(23) Frisch, M. J.; Trucks, G. W.;. Schlegel, H. B; Scuseria, G. E.; Robb, M. A.; Cheeseman, J. R.; Scalmani, G.; Barone, V.; Mennucci, B.; Petersson, G. A.; Nakatsuji, H.; Caricato, M.; Li, X.; Hratchian, H. P.; Izmaylov, A. F.; Bloino, J.; Zheng, G.; Sonnenberg, J. L.; Hada, M.; Ehara, M.; Toyota, K.; Fukuda, R.; Hasegawa, J.; Ishida, M.; Nakajima, T.; Honda, Y.; Kitao, O.; Nakai, H.; Vreven, T.; Montgomery, J. A., Jr.; Peralta, J. E.; Ogliaro, F.; Bearpark, M.; Heyd, J. J.; Brothers, E.; Kudin, K. N.; Staroverov, V. N.; Keith, T.; Kobayashi, R.; Normand, J.; Raghavachari, K.; Rendell, A.; Burant, J. C.; Iyengar, S. S.; Tomasi, J.; Cossi, M.; Rega, N.; Millam, N. J.; Klene, M.; Knox, J. E.; Cross, J. B.; Bakken, V.; Adamo, C.; Jaramillo, J.; Gomperts, R.; Stratmann, R. E.; Yazyev, O.; Austin, A. J.; Cammi, R.; Pomelli, C.; Ochterski, J. W.; Martin, R. L.; Morokuma, K.; Zakrzewski, V. G.; Voth, G. A.; Salvador, P.; Dannenberg, J. J.; Dapprich, S.; Daniels, A. D.; Farkas, O.; Foresman, J. B.; Ortiz, J. V.; Cioslowski, J.; Fox, D. J. *Gaussian 09*, Revision D.01; Gaussian, Inc.: Wallingford, CT, 2013.

(24) Andersson, K.; Malmqvist, P.-Å.; Roos, B. O. *J. Chem. Phys.* **1992**, *96*, 1218.

(25) Borden, W. T.; Davidson, E. R. *Acc. Chem. Res.* **1996**, *29*, 67.

(26) Aquilante, F.; De Vico, L.; Ferré, N.; Ghigo, G.; Malmqvist, P.-Å; Neogrády, P.; Pedersen, T. B.; Pitonak, M.; Reiher, M.; Roos, B. O.; Serrano-Andrés, L.; Urban, M.; Veryazov, V.; Lindh, R. *J. Comput. Chem.* **2010**, *31*, 224. Veryazov, V.; Widmark, P.-O.; Serrano-Andres, L.; Lindh, R.; Roos, B. O. *Int. J. Quantum Chem.* **2004**, *100*, 626. Karlström, G.; Lindh, R.; Malmqvist, P.-Å.; Roos, B. O.; Ryde, U.; Veryazov, V.; Widmark, P.-O.; Cossi, M.; Schimmelpfennig, B.; Neogrády, P.; Seijo, L. *Comput. Mater. Sci.* **2003**, *28*, 222.

(27) Yamaguchi, K.; Jensen, F.; Dorigo, A.; Houk, K. N. *Chem. Phys. Lett.* **1988**, *149*, 537.

(28) (a) Franck, J.; Dymond, E. G. *Trans. Faraday Soc.* **1926**, *21*, 536. (b) Condon, E. *Phys. Rev.* **1926**, *28*, 1182.

(29) The simulation in Figure 2 allows the vibrational excitations in forming the lowest singlet and triplet states of **TOTMB** from the lowest doublet state of $\mathbf{TOTMB}^{\bullet-}$ to be assigned. These assignments are provided in Figure S2 of the Supporting Information.

(30) Mozhayskiy, V. A.; Krylov, A. I. *ezSpectrum*, version 3.0; University of Southern California: Los Angeles, CA; http://iopenshell.usc.edu/downloads.

(31) (a) Kupka, H.; Cribb, P. *J. Chem. Phys.* **1986**, *85*, 1303. (b) Berger, R.; Fischer, C.; Klessinger, M. *J. Phys. Chem. A* **1998**, *102*, 7157. (c) Duschinsky, F. *Acta Physicochim. USSR* **1937**, *7*, 551.

(32) Schiedt, J.; Weinkauf, R. *J. Chem. Phys.* **1999**, *110*, 304.

(33) Review: Bally, T.; Borden, W. T. In *Reviews in Computational Chemistry*; Lipowitz, K. B., Boyd, D. B., Eds.; Wiley: New York, 1999; Vol. *13*, pp 1−99.

(34) The occupation numbers of the $b_{2g}$ and $b_{3u}$ MOs in the TCSCF wave function are also the same in **TOTMB** and **TMB**.

(35) Comparison of the calculated spin densities in the triplet states of **TOTMB** and **TMB** also shows that the four oxygens in **TOTMB** increase the localization of the unpaired electrons at C3 and C6 and decrease the amount of negative spin density present at C1, C2, C4, and C5. See Figure S6 of the SI for comparisons of the calculated [UB3LYP and (10/10)CASSCF] spin densities in **TOTMB** and **TMB**.



DOI: 10.1021/jacs.5b04416
*J. Am. Chem. Soc.* 2015, 137, 9094−9099